Published in final edited form as:
*Cancer Res*. 2009 October 1; 69(19): 7662–7671. doi:10.1158/0008-5472.CAN-09-1693.

# The IGF-1 Receptor Targeting Antibody, CP-751,871, Suppresses Tumor-Derived VEGF and Synergizes with Rapamycin in Models of Childhood Sarcoma

**Raushan T. Kurmasheva**[1], **Lorina Dudkin**[1], **Catherine Billups**[2], **Larisa V. Debelenko**[3], **Christopher L. Morton**[1], and **Peter J. Houghton**[1]

[1]Department of Molecular Pharmacology, St. Jude Children's Research Hospital

[2]Department of Biostatistics, St. Jude Children's Research Hospital

[3]Department of Pathology, St. Jude Children's Research Hospital

## Abstract

Signaling through the type 1 insulin-like growth factor receptor (IGF-1R) occurs in many human cancers, including childhood sarcomas. As a consequence, targeting the IGF-1R has become a focus for cancer drug development. We examined the antitumor activity of CP-751,871, a human antibody that blocks IGF-1R ligand binding, alone and in combination with rapamycin against sarcoma cell lines *in vitro* and xenograft models *in vivo*. In Ewing sarcoma (EWS) cell lines CP751,871 inhibited growth poorly (<50%), but prevented rapamycin-induced hyperphosphorylation of AKT(Ser473) and induced greater than additive apoptosis. Rapamycin treatment also increased secretion of IGF-1 resulting in phosphorylation of IGF-1R (Tyr1136) that was blocked by CP751,871. In vivo CP-751,871, rapamycin or the combination waere evaluated against EWS, osteosarcoma and rhabdomyosarcoma xenografts. CP751871 induced significant growth inhibition (EFS(T/C) >2) in four models. Rapamycin induced significant growth inhibition (EFS(T/C) >2) in nine models. Although neither agent given alone caused tumor regressions. in combination these agents had greater than additive activity against 5/13 xenografts and induced complete remissions (CR) in one model each of rhabdomyosarcoma and Ewing sarcoma, and in three of four osteosarcoma models. CP751,871 caused complete IGF-1R downregulation, suppression of AKT phosphorylation and dramatically suppressed tumor-derived VEGF in some sarcoma xenografts. Rapamycin treatment did not markedly suppress VEGF in tumors and synergized only in tumor lines where VEGF was dramatically inhibited by CP751,871. These data suggest a model in which blockade of IGF-1R suppresses tumor-derived VEGF to a level where rapamycin can effectively suppress the response in vascular endothelial cells.

## Introduction

Deregulated insulin-like growth factor signaling through the type-1 receptor (IGF-1R) appears common to many childhood solid tumors and offers an important molecular target for developmental therapeutic. For example, the alveolar subtype of rhabdomyosarcoma is associated with increased IGF-1R (1). For the embryonal rhabdomyosarcoma, the loss of imprinting at the IGF-2 locus may be a primary genetic event for embryonal rhabdomyosarcoma (2,3). IGF-1R is a potent mediator of autocrine growth in Ewing sarcoma (4,5), and EWS-FLI1 silencing leads to increased levels of insulin-like growth

Corresponding Author: Peter J. Houghton, PhD, Department of Molecular Pharmacology, St. Jude Children's Research Hospital, 332 North Lauderdale St., Memphis, TN 38105, Voice: (901) 595-3440, Fax: (901) 595-4290, peter.houghton@stjude.org.

factor binding protein 3 gene (IGFBP-3), a major regulator of IGF-1 (6). Additionally, IGF-1 is a mitogen for osteosarcoma (7–9), neuroblastoma (10,11), brain tumors [including glioblastoma (12,13), astrocytoma (14), medulloblastoma (15)], Wilms tumor (16), and hepatocellular carcinoma (17).

IGF-1R has become a major focus for cancer therapeutics development with at least five fully human antibodies in adult phase I–III clinical trials (18–24). These agents show specificity for the IGF-1R although they may also inhibit chimeric receptors formed through heterodimerization with the insulin receptor (IN-R). In preclinical cancer models antibody-mediated down regulation of IGF-1R significantly retards growth of many tumors (25), and induces regressions when combined with cytotoxic agents (19,26). These results are consistent with the significant literature that implicates IGF-1 signaling in survival of cells exposed to different cellular stresses (22).

The macrocyclic lactone antibiotic, rapamycin (sirolimus), is a highly specific inhibitor of mTOR a conserved serine/threonine kinase. The role of mTOR Complex 1 (mTORC1) in tumorigenesis and survival has become apparent (27,28). Rapamycin inhibits the proliferation of many tumor cell lines *in vitro* including cell lines derived from childhood cancers (29), and shows significant antitumor activity against syngeneic tumor models (30), and against childhood cancer xenografts (31). Rapamycin induced significant differences in event free survival (EFS) distribution in 33 of 44 (75%) solid pediatric tumor xenografts, showing particular activity against sarcoma and leukemia models (31).

We have tested the strategy of combining rapamycin with a human IGF-1 receptor-targeting antibody, CP-751,871, against cell lines and a comprehensive panel of more advanced-staged xenograft models derived from childhood sarcomas. Rather surprisingly, our data demonstrate that in some sarcoma xenografts IGF-1R significantly regulates the level of VEGF and its transcription, whereas inhibition of mTORC1 has a minor effect on the level of VEGF in these sarcomas.

## Materials and Methods

### Cell lines and xenograft models

Ewing sarcoma cells and xenografts used in this study all express EWS/FLI1. The RMS cell lines and xenografts and OS xenografts have been described previously (32,33). Cell lines were cultured in RPMI-1640 supplemented with 10% fetal bovine serum (FBS).

### *In vitro* growth inhibition studies

For prolonged serum-free experiments, EWS cells were cultured in modified N2E medium (34), and allowed to attach overnight. Next day 1 or 5 μg/ml of CP-751,871 was added to the fresh media. After 4 days of incubation cell viability was assessed by Alamar Blue staining (Biosource, Carlsbad, CA).

### Western blotting

Tumor tissue samples were pulverized under liquid $N_2$, and extracted as described previously (35). Immunoblotting procedures have been previously reported (35,36). We used primary antibodies to β-actin (Santa Cruz Biotechnology, Santa Cruz, CA), GAPDH, ribosomal protein S6 (rpS6), phospho-rpS6 (Ser235/236), AKT, phospho-AKT(Ser473), IGF-1R and pIGF-1R(Tyr1131) (Cell Signaling, Beverly, MA). The 7-methyl-GTP sepharose pull-down assay was used to determine binding of eIF4G to eIF4E as described previously (35). Immunoreactive bands were visualized by using SuperSignal®

Chemiluminiscence substrate (Pierce, Rockford, IL) and Biomax™ MR and XAR film (Eastman Kodak Co.).

### ELISA assays

VEGF levels in culture were determined by ELISA as previously described (36). For determining IGF's and VEGF in tumor tissue, tumor sample lysates were prepared from tumor tissue pulverized under liquid $N_2$. 2 μg/ml protein was used to run ELISA assay according to manufacturer's instructions (R&D Systems, Minneapolis).

### Quantitative Real-time RT-PCR

Total RNA was extracted using TRI Reagent (Ambion, Austin, TX) and purified to remove contaminating DNA (DNA free kit, Ambion). Total RNA (1μg) was reverse transcribed with hexamer primers and M-MLV Reverse Transcriptase (Clontech, Mountain View, CA). Gene expression of human VEGF and GAPDH was quantified on a Taqman 7900HT Thermal Cycler using Taqman® Gene Expression Assays and Taqman® Universal PCR Master Mix with no AmpErase® UNG (Applied Biosystems, Foster City, CA). Real-time RT-PCR singleplex reactions, final volume of 50 μl per 3 μl cDNA diluted in RNase-free water, 25 μl Universal Master Mix, and 2.5μl of 20× Gene Expression Assay Mix. Amplification conditions were set up to 10 min at 95°C followed by 40 PCR cycles (15 sec at 95°C, 1 min at 60°C). The quantity of cDNA used in each reaction was normalized to GAPDH and expressed as a ratio of sample cDNA to GAPDH cDNA.

### Immunohistochemical Studies

Tumor tissue was immediately fixed in formalin and processed using standard histologic procedures. Sections were stained with hematoxylin and eosin (H&E) and immunostained with mouse monoclocal Ki-67 antigen antibody (clone MIB-1, DakoCytomation, Denmark) and rabbit polycloncal phospho-BAD(Ser112) antibody (Cell Signaling Technology, Danvers, MA), following deparaffinization and antigen retrieval. TUNEL assays were performed on the deparaffinized 4 μm sections using the Promega Dead End kit (ProMega, Madison, WI).

### *In vivo* tumor growth inhibition studies

CB17SC-M *scid*$^{-/-}$ female mice (Taconic Farms, Germantown NY), were used to propagate subcutaneously implanted sarcomas. All mice were maintained under barrier conditions and experiments were conducted using protocols and conditions approved by the institutional animal care and use committee. Tumor volumes ($cm^3$) and tumor responses were determined as previously described (37) (see Supplemental response definitions).

### Statistical Methods

The exact log-rank test, as implemented using Proc StatXact for SAS®, was used to compare event-free survival distributions between treatment and control groups and between combinations and respective single-agent treatment groups. P-values were two-sided and both unadjusted and Bonferroni adjusted p-values were presented for multiple comparisons.

### Drugs and Formulation

Rapamycin was purchased from LC Laboratories, and CP-751,871 was generously provided by Bruce Cohen and James Christensen (Pfizer, Groton and San Diego). Mice received rapamycin (5 mg/kg) daily × 5 i.p. per week for up to 12 consecutive weeks. CP-751,871 was administered by i.p. injection at 0.5 mg or 0.25 mg per mouse twice weekly for up to 4 weeks.

## Results

### In vitro studies with EWS cells

Maximum growth inhibition of Ewing sarcoma cell lines growing in serum-containing medium was achieved at 1 μg/ml CP-751,871, a monoclonal antibody that targets the human IGF-1R to prevent ligand binding (19). Maximum inhibition of growth was 50% (ES-1 cells) whereas under these growth conditions ES-7 and ES-8 cell lines were essentially resistant to CP-751,871 (Figure 1A). Previously we reported that inhibition of mTORC1 signaling by rapamycin induced apoptosis in sarcoma cells in serum-free medium (34). To determine whether concomitant inhibition of IGF-1R and mTORC1 signaling enhanced cell death compared to rapamycin alone, EWS cells were grown under serum-free conditions with or without rapamycin, CP-751,871 or with the combination of these agents. Apoptosis was determined by FACs analysis as previously described (34). CP-751,871 alone induced apoptosis in only ES-8 cells, whereas approximately 32% of EW-8 cells were determined to be apoptotic after 4 days of rapamycin treatment. Combined treatment with rapamycin and CP-751,871 was supra additive in each EWS cell line examined, increasing the nonviable fraction in all cell lines tested (Suppl. Table 1).

Several studies have shown rapamycin-induced hyperphosphorylation of AKT (Ser473). The putative mechanism is through inhibition of S6K1, downstream of mTORC1, and relief of the negative feedback on IRS-1 (36,38,39). As shown in Figure 1B, rapamycin induced a robust increase in AKT(Ser473) phosphorylation in EWS cells and this was blocked by CP-751,871. Rapamycin also induced hyperphosphorylation of IGF-1R(Tyr1131), suggesting receptor activation by ligand. For all Ewing cell lines, rapamycin significantly increased IGF-1 secreted into the medium, suggesting that cells compensate for mTORC1 inhibition by inducing this survival factor, Figure 1C. CP-751,871 alone increased IGF-1 i n E S-1 and ES-2 cell lines only, whereas the combination of CP-751,871 with rapamycin was additive in ES-1, ES-8 and EW-8 lines.

### Combined inhibition of IGF-1R and mTORC1 inhibits VEGF

Combined inhibition of AKT and mTORC1 synergistically suppresses VEGF secretion by rhabdomyosarcoma (RMS) and neuroblastoma cells in culture (36). To determine whether simultaneous blockade of IGF-1R and mTORC1 could achieve similar effects on VEGF, cells were incubated for 24 hr under normoxia (21% $O_2$) or hypoxia (1% $O_2$) without or with CP-751,871, rapamycin or both agents. At the end of the incubation period medium was harvested and VEGF/$10^6$ cells determined. As shown in Figure 1D under normoxic conditions the combination of inhibitors was essentially additive in reducing VEGF levels in most EWS and RMS cells, whereas CP-751,871 did not enhance the effect of rapamycin in reducing VEGF levels in ES-7 or Rh36 cells. Similar results were obtained under hypoxic conditions where the combination significantly reduced hypoxia-driven increases in levels of VEGF.

### In vivo antitumor activity

To determine whether this combination was therapeutically useful we examined the antitumor activity of the individual agents, and the combination of CP-751,871 with rapamycin in a series of xenograft models representing EWS (n=6; Figure 2A), osteosarcoma (OS; n=4; Figure 2B) and RMS (n=2). A complete summary of results is shown in Supplemental Table 2. CP-751,871 was administered i.p. twice weekly for a planned 4 weeks only, whereas rapamycin was administered daily for 5 days per week for up to 12 consecutive weeks. CP-751,871 administered at 0.5 mg/mouse or 0.25 mg/mouse had essentially identical antitumor activity (Supplemental Table 2).

Rapamycin, CP-751,871 or the combination had low or intermediate antitumor activity against ES-1, ES-7 or EW-8 xenografts (Supplemental Table 3). Of note the combination of rapamycin and CP-751,871 induced complete regressions (CR) of EW-5 xenografts (18/18 CRs, Supplemental Table 2). Kaplan-Meier EFS estimates and tumor growth curves for the EWS models are shown in Figure 2. Against the osteosarcoma models, CP-751,871 induced regressions of OS-1, and significantly retarded growth of OS-9 but was less effective against OS-2 or OS-17 xenografts (**Figure B**, Supplemental Table 2). Rapamycin was most active against OS-2 and OS-17 xenografts. However, the combination induced CR in all but OS-17 tumors where it significantly inhibited growth over the 12-week period of observation.

Although rapamycin significantly inhibited growth of Rh18 RMS xenografts, it caused few regressions (2/10 CR) whereas the combination induced CR in 9 of 10 mice (Supplemental Table 2). The combination had essentially additive activity against Rh30 tumors, but induced no regressions, consistent with the data of Cao et al (40).

## Pharmacodynamic and Morphologic studies

Downstream substrates for IGF-1R [pAKT(Ser473)] and mTORC1 [pS6(Ser235/6)] were examined in tumor tissues 25 and 169 hr after initiating therapy with CP-751,871, rapamycin or the combination. Tumors were harvested 1 hr after the final dose of rapamycin.

**Ewing sarcoma xenografts—**Three tumors (ES-1, ES-7, EW-8) showed progressive growth, and were considered as failing each therapy (Figure 3A). Three other Ewing sarcoma models showed some sensitivity to rapamycin (ES-2, ES-8) or both agents (EW-5), Figure 3B. For example, in the ES-1 model neither single agent significantly retarded growth whereas the combination was somewhat more effective over the first 7 days of treatment (mean 44% growth inhibition). For all ES tumors failure to respond to CP-751,871 was characterized by a failure to down regulate IGF-1R, to suppress pAKT levels, or to completely suppress pS6. In contrast, EW-5 xenografts were growth inhibited (~94% by day 7), and showed dramatic down regulation of IGF-1R, and decreased pAKT and diminished pS6 over this time period.

Synergistic antitumor activity of CP-751,871 combined with rapamycin in EW-5 was not paralleled by a significant change in the pharmacodynamic markers over those seen with each agent individually. Morphologic examination of EW-5 tumors at 169 hr demonstrated a dramatic loss of tumor cells and subtotal replacement of the tumor implantation bed by adipose tissue. This was due to both cessation of proliferation (~10 fold decrease of percentage of Ki67-positive tumor cells), and induction of apoptosis (as confirmed by TUNEL assay) in combination-treated tumors (Figure 3C).

**Osteosarcoma xenografts—**Compared to either single agent, the combination of CP-751,871 with rapamycin extended EFS in all OS tumor models and increased the fraction of mice that were in CR at week 12 (Supplemental Table 2). CP-751,871 alone induced regressions of some OS-1 xenografts, and retarded the growth of OS-2 and OS-9 tumors. CP751,871 caused down regulation of IGF-1R in OS-1 and OS-2 models, but suppressed p-AKT in OS-1, OS-2 and OS-9 tumors, despite failing to down regulate IGF-1R in the latter model (Figure 4). Antibody treatment effectively suppressed rapamycin-induced hyperphosphorylation of AKT (Ser473) in all OS models except OS-17.

Similar pharmacodynamic changes in OS-1 tumors were obtained with the combined treatment with rapamycin and CP-751,871, although the combination was more efficacious with 11/13 mice being in CR compared to 2/20 CP-751,871-treated mice at the end of the observation period (12 weeks). Similar pharmacodynamic effects were detected in OS-2

tumors treated with CP-751,871, although these xenografts progressed during the first 7 d of treatment. OS-2 tumors treated with the combination of CP-751,871 and rapamycin regressed, but changes in pharmacodynamic parameters did not distinguish between the effects of CP-751,871, rapamycin or the combination treatment (Figure 4). However, by immunohistochemical staining, the combination of CP-751,871 and rapamycin had greater than additive activity in reducing proliferation in OS-9 xenografts, as determined by Ki-67 staining, (Supplemental Figure 1)

## Therapy-induced changes in tumor-derived VEGF

As shown in Figure 1, rapamycin and CP-751,871 each reduced secretion of VEGF by EWS cells *in vitro*. To determine whether changes of tumor-derived VEGF correlated with the antitumor effect of each agent, alone or in combination, levels were determined by a human-specific VEGF ELISA.

**Ewing sarcoma xenografts—**Drug-induced changes in VEGF are shown for EWS (Figure 5A). In contrast to the relatively modest effect measured *in vitro*, CP-751,871 significantly and markedly suppressed VEGF levels within 25 hr in ES-1, EW-5, and EW-8 models ($P<0.002$). Of note, levels of VEGF in control tumors had increased by day 7, probably reflecting their increase in mass and increased hypoxic regions within these larger tumors. On day 7 of treatment levels of VEGF were significantly decreased from controls in ES-1, EW-5 and EW-8 xenograft models, with extremely low levels (<10ng/ml) detected in EW-5 tumors. In contrast to CP751,871, rapamycin treatment had a small effect on decreasing VEGF at 25 hr reaching significance in only ES-2, EW-5 and EW-8 xenografts ($P<0.05$). On day 7 treatment with rapamycin only decreased VEGF significantly in ES-8 tumors, whereas rapamycin stimulated tumor-associated VEGF in ES-1 at both examined time points.

**Osteosarcoma xenografts—**The basal level of tumor-associated VEGF was low in OS-1, OS-2 and OS-9 tumors, being 31, 0.33 and 51 ng/mg protein respectively, whereas the basal level of VEGF associated with OS-17 xenografts was 251 ng/mg protein. CP751,871 treatment significantly decreased VEGF levels in OS-1, and OS-9 xenografts ($P< 0.002$) whereas VEGF was not detected in OS-2 tumors at 25 hr. In contrast CP751,871 increased VEGF associated with OS-17 tumors ($P=0.05$) at this time point. At 169 hr of treatment CP751,871 completely suppressed VEGF in OS-1, OS-2 and OS-9 xenografts, whereas the levels in OS-17 were significantly reduced from that in control tumors ($P<0.0001$), Figure 5B. Rapamycin treatment did not significantly decrease tumor-associated VEGF levels at 25 hr or 169 hr in any OS tumor line. However, at 169 hr rapamycin treatment was associated with significantly elevated levels of VEGF in OS-1 ($P=0.036$) and OS-17 ($P=0.0001$) xenografts. Treatment with the combination of CP751,871 and rapamycin significantly decreased tumor-associated VEGF at both time points examined in all models ($P< 0.0001$) except OS-17 where the decrease did not reach statistical significance ($P=0.0503$) at the 25 hr determination.

## CP-751,871 rapidly suppresses VEGF transcription

To determine the mechanism by which CP-751,871 suppressed tumor-derived VEGF, RNA was extracted from control or CP-751,871-treated tumors and VEGF transcripts were determined by quantitative RT-PCR as described in Materials and Methods. Tumors from the 25 hr time point were used, rather than 169 hr into treatment, as marked tumor regression had occurred at the latter time. Three CP-751,871 non-responding tumors (ES-7, ES-8, OS-17) and two responding tumors (EW-5 and OS-1) were analyzed. As shown in Figure 6, decreased VEGF transcripts determined by RT-PCR, paralleled decreased levels of VEGF determined by ELISA 25 hr after the first dose of CP-751,871.

## Discussion

Panels of childhood cancer xenografts (32), accurately recapitulate the expression profiles of their respective clinical histotypes (41,42). Reference to this Pediatric Preclinical Testing Program (PPTP) Affymetrix database[1] revealed expression of IGF-1R was upregulated in most EWS, OS and RMS models, as was expression of either IGF-1 or IGF-2. Relative secretion of IGF-1 or IGF-2 was confirmed in cell lines using an ELISA, showing that EWS lines secrete more IGF-1 whereas RMS secrete far higher levels of IGF-2 than IGF-1 (data not shown). However, inhibition of proliferation for EWS or RMS (data not shown) cells *in vitro* was relatively modest when cells were exposed to CP-751,871. Similar results were reported for another IGF-1R-targeting antibody, SCH717454 (43). As reported previously (36,38,39) rapamycin-induced phosphorylation of AKT(Ser473) in the sarcoma cell lines studied. In part, increased activation of AKT is a consequence of IRS-1 stabilization when mTORC1 signaling is attenuated. However, rapamycin also increased phosphorylation of the IGF-1R, and increased secretion of IGF-1 in EWS cell lines. CP-751,871 blocked IGF-mediated rescue and enhanced rapamycin-induced apoptosis in all EWS and RMS cell lines under serum-free conditions. Further, inhibition of two points in this signaling cascade was found to be additive in suppressing secretion of VEGF (36). Consistent with these observations, combining rapamycin and CP-751,871 decreased secretion of VEGF in most Ewing sarcoma cell lines.

The antitumor activity of rapamycin, CP-751,871 and the combination of agents was tested against twelve sarcoma models using response criteria developed for the PPTP (supplemental response definitions). As a single agent CP-751,871 exhibited intermediate activity using event free survival (EFS(T/C) ≥ 2.0) in EW-5, OS-1 and OS-9 xenografts only. For EWS xenografts the highest level of IGF-1R was in the most sensitive line (EW-5; Supplemental Figure 2), however, there was no strict correlation between IGF-1R levels and CP-751,871 induced growth inhibition. CP-751,871 induced similar growth inhibition against Rh30, Rh18 and OS-17 xenografts [EFS(T/C) 1.4 – 1.6] that have quite different receptor levels. Hence the correlation reported for sarcoma cell lines determined *in vitro* (40) appears less robust *in vivo*.

The combination of CP-751,871 with rapamycin was supra additive against EW-5, and OS-9 models. In addition, for OS-1 osteosarcoma the combination induced 10/10 CRs whereas the CP-751,871 alone induced 4/9 CRs, and in OS-2 the combination resulted in PR or CR for all tumors compared to progressive disease in the single agent groups. CP-751,871 significantly inhibited Rh18 xenografts (EFS(T/C) =1.6, p=0.0015), however while the combination inhibited growth similar to that of single agent rapamycin (EFS(T/C) > 15.5) it induced 9 of 10 CRs compared to only 2 of 10 for rapamycin alone. For Rh30 xenografts the combination EFS(T/C) was essentially additive for the two individual agents, with no tumor regressions. Using objective response criteria, combining CP-751,871 with rapamycin clearly increased the objective response rate in EW-5, OS-1, OS-2, OS-9 and Rh18 xenograft models compared to either monotherapy.

Identifying pharmacodynamic markers of tumor response to rapalogs has proven to be difficult in clinical trials (44). Specifically, markers of decreased mTORC1 signaling tend to be inhibited irrespective of tumor response. We attempted to identify pharmacodynamic markers in tumor tissue that ‘tracked’ with the antitumor activity of both single agents and the combination. The effect of CP-751,871 on down regulating IGF-1R was highly tumor specific. Rapid loss of receptor was found for EW-5, OS-1 and OS-2 xenografts, whereas IGF-1R was not diminished in many other tumors (ES-7, EW-8, ES-8, OS-9). However,

[1]http://pptp.stjude.org/affyData.php?dir=/doc/affyData/Expression/CEL

immunoblotting, as used here, does not distinguish between membrane associated receptor, or internalized receptor that has not been degraded. Tumors where the combination of CP-751,871 and rapamycin was highly effective at causing tumor regression (OS-1, OS-2, OS-9, EW-5, Rh18) demonstrated complete suppression of pS6 and marked reduction in IGF-1R levels at 169 hr. The role for pAKT(Ser473) is less clear, as phosphorylation at 169 hr had returned to control levels in EW-5 and OS-2 tumors, despite these xenografts regressing on combination treatment. Rapamycin induced hyperphosphorylation of AKT(Ser473) at 25 hr and 169 hr in most tumor models, suggesting that irrespective of continued treatment with rapamycin that blocked mTORC1 signaling, mTORC2 signaling remained intact during this period. Notably, CP-751,871 blocked completely (ES-8, EW-5, OS-1, OS-9), or partially (OS-2, OS-17) rapamycin-induced hyperphosphorylation of AKT(Ser473). However, CP-751,871 also partially blocked rapamycin-induced pAKT(Ser473) in the ES-1 xenograft line that was poorly responsive to any therapy (EFS(T/C) < 2.0). Combination treatment also significantly decreased Ki67 staining in EW-5 and OS-9 xenografts, but increased the frequency of TUNEL-positive cells in EW-5 only.

Inhibition of mTORC1 signaling may have direct effect on cell proliferation and survival, or an indirect effect *via* inhibition of HIF-1α, thus reducing tumor-elicited VEGF. Conversely, PI3K/AKT signaling can induce tumor angiogenesis by regulating VEGF. This regulation occurs at both the mRNA and protein levels, and its regulation of VEGF mRNA appears to occur by both HIF-1α-dependent and -independent mechanisms (45) . Rapamycin may also exert direct effect on vascular endothelial cells, or vascular smooth muscle cells (46,47). Guba and colleagues (48) concluded that the antitumor activity of rapamycin was due to its antiangiogenic activity as rapamycin decreased production of VEGF and markedly inhibited response of vascular endothelial cells to stimulation by VEGF. In our study the pharmacodynamic markers for supra-additive activity for the combination were significant downregulation of IGF-1R and complete suppression of phospho-S6 for up to 169 hr. Most notably, within 25 hr of administration CP-751,871 induced a very marked decrease in VEGF in EW-5, OS-1, OS-2 and OS-9 xenografts and suppression of VEGF was maintained at 169 hr. Consistent with decreased VEGF in tumor tissue, levels of VEGF transcripts were reduced only in tumors where CP-751,871 suppressed levels of VEGF within 25 hr of treatment. In contrast to treatment with CP-751,871, rapamycin treatment stimulated tumor-derived VEGF levels above control tumor levels at 25 hr (ES-1) or 169 hr of treatment (ES-1, ES-7, OS-9), and partly antagonized the suppression of VEGF by CP-751,871 in ES-1, EW-8 and Rh30 xenografts. Importantly, suppression of tumor-derived VEGF correlated with marked downregulation of IGF-1R and decreased pAKT induced by CP-751,871. Of note, only in these tumors (EW-5, OS-1, OS-2, OS-9) was there a marked increase in the frequency of objective tumor responses and maintained CRs when CP-751,871 was combined with rapamycin.

Our results suggests that under conditions of tumor growth *in vivo*, IGF-1R signaling significantly regulates VEGF production despite continued evidence of mTORC1 activity (as shown by maintained phospho-S6). Synergy of the rapamycin-CP-751,871 combination occurred in tumors with low endogenous VEGF (< 13 ng/mg protein, EW-5, Rh18, OS-2) or where CP-751,871 dramatically decreased VEGF (OS-1, OS-9). In contrast to CP-751,871, rapamycin had less effect on tumor-derived VEGF, and partially antagonized CP-751,871, despite the combination demonstrating synergistic antitumor activity. Thus, suppression of tumor-derived VEGF is only part of the mechanism, as CP-751,871 alone did not cause tumor regressions, except in OS-1 xenografts. This suggests a model in which one agent (CP-751,871) predominantly suppresses the ability of tumors to synthesize VEGF, which in itself is insufficient to completely suppress tumor growth, while the other agent (rapamycin) blocks the response to VEGF in cells of the vascular compartment. This model predicts that tumors with the lowest basal levels of VEGF would be the most sensitive to rapamycin.

Indeed the two most rapamycin-sensitive xenograft lines Rh18, and OS-2, [(EFS (T/C) >15.5 and >6.6, respectively] had the lowest basal levels of VEGF, although OS-17 tumors were somewhat rapamycinsensitive (EFS (T/C) = 5.5) but had extremely high VEGF levels. Based on these data, it appears essential to reduce tumor levels of VEGF to a very low level through inhibiting IGF-1R in order for rapamycin to effectively synergize. If this model is correct, IGF-1R blockade (to reduce VEGF levels) in combination with small molecule inhibitor of VEGF receptors or bevacizumab, may also be an effective strategy for treatment of these sarcomas.

## Supplementary Material

Refer to Web version on PubMed Central for supplementary material.

## Acknowledgments

We thank Claire Boltz, Shea Mercer, Jeri Carol Crumpton, Doris Phelps, Dorothy Bush and Charlene Henry for excellent technical assistance.

This work was supported by USPHS grants CA23099, CA77776 and CA21675 (Cancer Center Support Grant), and by American, Lebanese, Syrian Associated Charities (ALSAC).

## References

1. Ayalon D, Glaser T, Werner H. Transcriptional regulation of IGF-I receptor gene expression by the PAX3-FKHR oncoprotein. Growth Horm IGF Res 2001;11:289–297. [PubMed: 11735247]
2. Fukuzawa R, Umezawa A, Ochi K, Urano F, Ikeda H, Hata J. High frequency of inactivation of the imprinted H19 gene in "sporadic" hepatoblastoma. International journal of cancer 1999;82:490–497.
3. Minniti CP, Tsokos M, Newton WA Jr, Helman LJ. Specific expression of insulin-like growth factor-II in rhabdomyosarcoma tumor cells. Am J Clin Pathol 1994;101:198–203. [PubMed: 8116575]
4. Scotlandi K, Benini S, Nanni P, et al. Blockage of insulin-like growth factor-I receptor inhibits the growth of Ewing's sarcoma in athymic mice. Cancer research 1998;58:4127–4131. [PubMed: 9751624]
5. Scotlandi K, Benini S, Sarti M, et al. Insulin-like growth factor I receptor-mediated circuit in Ewing's sarcoma/peripheral neuroectodermal tumor: a possible therapeutic target. Cancer research 1996;56:4570–4574. [PubMed: 8840962]
6. Prieur A, Tirode F, Cohen P, Delattre O. EWS/FLI-1 silencing and gene profiling of Ewing cells reveal downstream oncogenic pathways and a crucial role for repression of insulin-like growth factor binding protein 3. Molecular and cellular biology 2004;24:7275–7283. [PubMed: 15282325]
7. Pollak M, Richard M. Suramin blockade of insulinlike growth factor I-stimulated proliferation of human osteosarcoma cells. Journal of the National Cancer Institute 1990;82:1349–1352. [PubMed: 2166171]
8. Bostedt KT, Schmid C, Ghirlanda-Keller C, Olie R, Winterhalter KH, Zapf J. Insulin-like growth factor (IGF) I down-regulates type 1 IGF receptor (IGF 1R) and reduces the IGF I response in A549 non-small-cell lung cancer and Saos-2/B-10 osteoblastic osteosarcoma cells. Experimental cell research 2001;271:368–377. [PubMed: 11716549]
9. MacEwen EG, Pastor J, Kutzke J, et al. IGF-1 receptor contributes to the malignant phenotype in human and canine osteosarcoma. Journal of cellular biochemistry 2004;92:77–91. [PubMed: 15095405]
10. El-Badry OM, Helman LJ, Chatten J, Steinberg SM, Evans AE, Israel MA. Insulin-like growth factor II-mediated proliferation of human neuroblastoma. The Journal of clinical investigation 1991;87:648–657. [PubMed: 1991849]
11. Weber A, Huesken C, Bergmann E, Kiess W, Christiansen NM, Christiansen H. Coexpression of insulin receptor-related receptor and insulin-like growth factor 1 receptor correlates with enhanced

apoptosis and dedifferentiation in human neuroblastomas. Clin Cancer Res 2003;9:5683–5692. [PubMed: 14654552]

12. Sandberg AC, Engberg C, Lake M, von Holst H, Sara VR. The expression of insulin-like growth factor I and insulin-like growth factor II genes in the human fetal and adult brain and in glioma. Neurosci Lett 1988;93:114–119. [PubMed: 3211366]
13. Resnicoff M, Li W, Basak S, Herlyn D, Baserga R, Rubin R. Inhibition of rat C6 glioblastoma tumor growth by expression of insulin-like growth factor I receptor antisense mRNA. Cancer Immunol Immunother 1996;42:64–68. [PubMed: 8625368]
14. Antoniades HN, Galanopoulos T, Neville-Golden J, Maxwell M. Expression of insulin-like growth factors I and II and their receptor mRNAs in primary human astrocytomas and meningiomas; in vivo studies using in situ hybridization and immunocytochemistry. International journal of cancer 1992;50:215–222.
15. Del Valle L, Enam S, Lassak A, et al. Insulin-like growth factor I receptor activity in human medulloblastomas. Clin Cancer Res 2002;8:1822–1830. [PubMed: 12060623]
16. Hirschfeld S, Helman L. Diverse roles of insulin-like growth factors in pediatric solid tumors. In Vivo 1994;8:81–90. [PubMed: 8054516]
17. Scharf JG, Braulke T. The role of the IGF axis in hepatocarcinogenesis. Horm Metab Res 2003;35:685–693. [PubMed: 14710347]
18. Braczkowski R, Schally AV, Plonowski A, et al. Inhibition of proliferation in human MNNG/HOS osteosarcoma and SK-ES-1 Ewing sarcoma cell lines in vitro and in vivo by antagonists of growth hormone-releasing hormone: effects on insulin-like growth factor II. Cancer 2002;95:1735–1745. [PubMed: 12365022]
19. Cohen BD, Baker DA, Soderstrom C, et al. Combination therapy enhances the inhibition of tumor growth with the fully human anti-type 1 insulin-like growth factor receptor monoclonal antibody CP-751,871. Clin Cancer Res 2005;11:2063–2073. [PubMed: 15756033]
20. Wang Y, Hailey J, Williams D, et al. Inhibition of insulin-like growth factor-I receptor (IGF-IR) signaling and tumor cell growth by a fully human neutralizing anti-IGF-IR antibody. Molecular cancer therapeutics 2005;4:1214–1221. [PubMed: 16093437]
21. Guerreiro AS, Boller D, Doepfner KT, Arcaro A. IGF-IR: potential role in antitumor agents. Drug News Perspect 2006;19:261–272. [PubMed: 16941048]
22. Kurmasheva RT, Houghton PJ. IGF-I mediated survival pathways in normal and malignant cells. Biochimica et biophysica acta 2006;1766:1–22. [PubMed: 16844299]
23. Sachdev D, Yee D. Inhibitors of insulin-like growth factor signaling: a therapeutic approach for breast cancer. J Mammary Gland Biol Neoplasia 2006;11:27–39. [PubMed: 16947084]
24. Sachdev D, Yee D. Disrupting insulin-like growth factor signaling as a potential cancer therapy. Molecular cancer therapeutics 2007;6:1–12. [PubMed: 17237261]
25. Sachdev D, Li SL, Hartell JS, Fujita-Yamaguchi Y, Miller JS, Yee D. A chimeric humanized single-chain antibody against the type I insulin-like growth factor (IGF) receptor renders breast cancer cells refractory to the mitogenic effects of IGF-I. Cancer research 2003;63:627–635. [PubMed: 12566306]
26. Goetsch L, Gonzalez A, Leger O, et al. A recombinant humanized anti-insulin-like growth factor receptor type I antibody (h7C10) enhances the antitumor activity of vinorelbine and anti-epidermal growth factor receptor therapy against human cancer xenografts. International journal of cancer 2005;113:316–328.
27. Wullschleger S, Loewith R, Hall MN. TOR signaling in growth and metabolism. Cell 2006;124:471–484. [PubMed: 16469695]
28. Bjornsti MA, Houghton PJ. The TOR pathway: a target for cancer therapy. Nat Rev Cancer 2004;4:335–348. [PubMed: 15122205]
29. Dilling MB, Dias P, Shapiro DN, Germain GS, Johnson RK, Houghton PJ. Rapamycin selectively inhibits the growth of childhood rhabdomyosarcoma cells through inhibition of signaling via the type I insulin-like growth factor receptor. Cancer research 1994;54:903–907. [PubMed: 7508822]
30. Houchens DP, Ovejera AA, Riblet SM, Slagel DE. Human brain tumor xenografts in nude mice as a chemotherapy model. Eur J Cancer Clin Oncol 1983;19:799–805. [PubMed: 6683650]

31. Houghton PJ, Morton CL, Kolb EA, et al. Initial testing (stage 1) of the mTOR inhibitor rapamycin by the pediatric preclinical testing program. Pediatr Blood Cancer 2008;50:799–805. [PubMed: 17635004]
32. Houghton PJ, Morton CL, Tucker C, et al. The pediatric preclinical testing program: Description of models and early testing results. Pediatr Blood Cancer. 2006
33. Meyer WH, Houghton JA, Houghton PJ, Webber BL, Douglass EC, Look AT. Development and characterization of pediatric osteosarcoma xenografts. Cancer research 1990;50:2781–2785. [PubMed: 2328504]
34. Thimmaiah KN, Easton J, Huang S, et al. Insulin-like growth factor I-mediated protection from rapamycin-induced apoptosis is independent of Ras-Erk1-Erk2 and phosphatidylinositol 3'-kinase-Akt signaling pathways. Cancer research 2003;63:364–374. [PubMed: 12543789]
35. Dudkin L, Dilling MB, Cheshire PJ, et al. Biochemical correlates of mTOR inhibition by the rapamycin ester CCI-779 and tumor growth inhibition. Clin Cancer Res 2001;7:1758–1764. [PubMed: 11410517]
36. Kurmasheva RT, Harwood FC, Houghton PJ. Differential regulation of vascular endothelial growth factor by Akt and mammalian target of rapamycin inhibitors in cell lines derived from childhood solid tumors. Mol Cancer Ther 2007;6:1620–1628. [PubMed: 17483438]
37. Houghton PJ, Morton CL, Tucker C, et al. The pediatric preclinical testing program: description of models and early testing results. Pediatr Blood Cancer 2007;49:928–940. [PubMed: 17066459]
38. Shi Y, Yan H, Frost P, Gera J, Lichtenstein A. Mammalian target of rapamycin inhibitors activate the AKT kinase in multiple myeloma cells by up-regulating the insulin-like growth factor receptor/insulin receptor substrate-1/phosphatidylinositol 3-kinase cascade. Mol Cancer Ther 2005;4:1533–1540. [PubMed: 16227402]
39. O'Reilly KE, Rojo F, She QB, et al. mTOR inhibition induces upstream receptor tyrosine kinase signaling and activates Akt. Cancer Res 2006;66:1500–1508. [PubMed: 16452206]
40. Cao L, Yu Y, Darko I, et al. Addiction to elevated insulin-like growth factor i receptor and initial modulation of the AKT pathway define the responsiveness of rhabdomyosarcoma to the targeting antibody. Cancer research 2008;68:8039–8048. [PubMed: 18829562]
41. Whiteford CC, Bilke S, Greer BT, et al. Credentialing preclinical pediatric xenograft models using gene expression and tissue microarray analysis. Cancer Res 2007;67:32–40. [PubMed: 17210681]
42. Neale G, Su X, Morton CL, et al. Molecular characterization of the pediatric preclinical testing panel. Clin Cancer Res 2008;14:4572–4583. [PubMed: 18628472]
43. Kolb EA, Gorlick R, Houghton PJ, et al. Initial testing (stage 1) of a monoclonal antibody (SCH 717454) against the IGF-1 receptor by the pediatric preclinical testing program. Pediatr Blood Cancer 2008;50:1190–1197. [PubMed: 18260118]
44. Tabernero J, Rojo F, Calvo E, et al. Dose- and schedule-dependent inhibition of the mammalian target of rapamycin pathway with everolimus: a phase I tumor pharmacodynamic study in patients with advanced solid tumors. J Clin Oncol 2008;26:1603–1610. [PubMed: 18332469]
45. Arsham AM, Plas DR, Thompson CB, Simon MC. Akt and hypoxia-inducible factor-1 independently enhance tumor growth and angiogenesis. Cancer Res 2004;64:3500–3507. [PubMed: 15150104]
46. Humar R, Kiefer FN, Berns H, Resink TJ, Battegay EJ. Hypoxia enhances vascular cell proliferation and angiogenesis in vitro via rapamycin (mTOR)-dependent signaling. Faseb J 2002;16:771–780. [PubMed: 12039858]
47. Majumder PK, Febbo PG, Bikoff R, et al. mTOR inhibition reverses Akt-dependent prostate intraepithelial neoplasia through regulation of apoptotic and HIF-1-dependent pathways. Nat Med 2004;10:594–601. [PubMed: 15156201]
48. Guba M, von Breitenbuch P, Steinbauer M, et al. Rapamycin inhibits primary and metastatic tumor growth by antiangiogenesis: involvement of vascular endothelial growth factor. Nat Med 2002;8:128–135. [PubMed: 11821896]

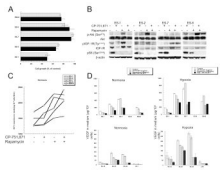

**Figure 1.**
*In vitro* studies with CP-751,871.

**A.** EWS cells were incubated in serum-containing medium ± CP-751,871 at 1 (black bars) or 5 μg/ml (stippled bars). Cell growth was determined by Alamar Blue staining after 4 d. Results are presented as percent control growth (mean ± SD. n=3).

**B.** EWS cells were incubated with CP-751,871 (1 μg/ml), rapamycin (100 ng/ml), the combination, or without drugs for 24 hr. Cell lysates were probed for total and phosphorylated IGF-1R, AKT, and S6. β-actin serves as a loading control.

**C.** EWS cells were incubated with CP-751,871 (1 μg/ml), rapamycin (100 ng/ml), the combination, or without drugs for 24 hr. IGF-1 in media was determined by ELISA and expressed as ng/$10^6$ cells (mean, n=2).

**D.** EWS or RMS cells were grown under normoxic conditions (21% $O_2$) or hypoxic conditions (1% $O_2$) in the absence or presence of drugs. VEGF in media was determined by ELISA and expressed as pg/$10^6$ cells (Mean ± SD, n=3).

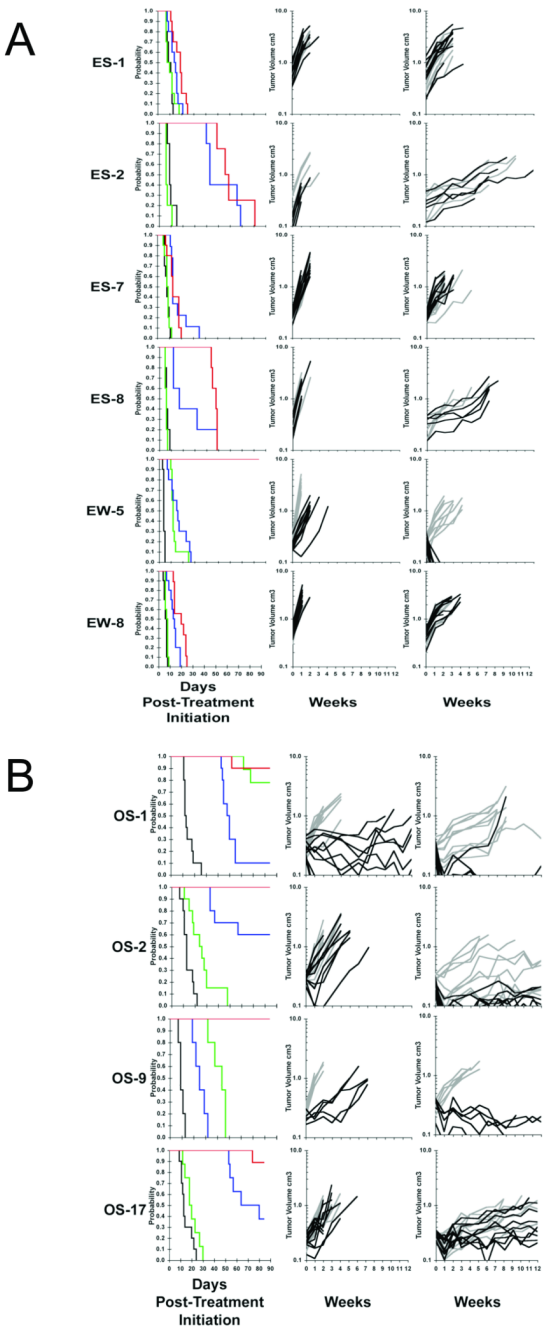


**Figure 2.**

**A.** Responses of Ewing sarcoma xenografts to CP-751,871, rapamycin or the combination treatment.

**B.** Responses of osteosarcoma xenografts to CP-751,871, rapamycin or the combination treatment.

Tumor-bearing mice were treated with CP-751,871 (0.25 mg/mouse twice weekly × 4). Rapamycin (5 mg/kg daily × 5 per week for up to 12 consecutive weeks) or the combination of CP-751,871 and rapamycin. Tumor diameters were measured weekly.

*Left panels*: Kaplan Meier event free survival (EFS). Control (black), CP-751,871 (green), rapamycin (blue) or CP-751,871 + rapamycin (red). Curves show the probability of mice being event-free (tumor volume < 4-fold that at initiation of treatment) against days post treatment initiation.
*Center panels*: Growth of individual tumors; Controls (light gray), CP-751,871 treated (black). *Right panels*: Growth of individual tumors; Rapamycin (light gray), CP-751,871 + rapamycin treated (black).

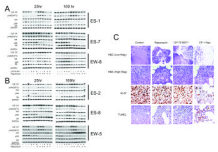

**Figure 3.**

Pharmacodynamic changes in EWS xenografts associated with treatment regimens. Mice received CP-751,871 (0.5 mg/mouse) twice weekly, rapamycin daily 5-days per week or the combination. Tumors were harvested 1 hr after the last dose of rapamycin, and snap-frozen in liquid $N_2$. Extracts were prepared from tumors and processed as described in Experimental Procedures. For each condition (control, CP-751,871, rapamycin or the combination) 3 independent tumors were used at each time point.

**A.** Non-responsive EWS xenografts.

**B.** EWS xenografts responding to at least one agent or the combination

**C.** Histology and immunohistochemistry of control EW-5 tumors or after 169 hr treatment with rapamycin, CP-751,871 or the combination. Tumor sections were stained for Ki-67, a marker for proliferation, and apoptosis (TUNEL).

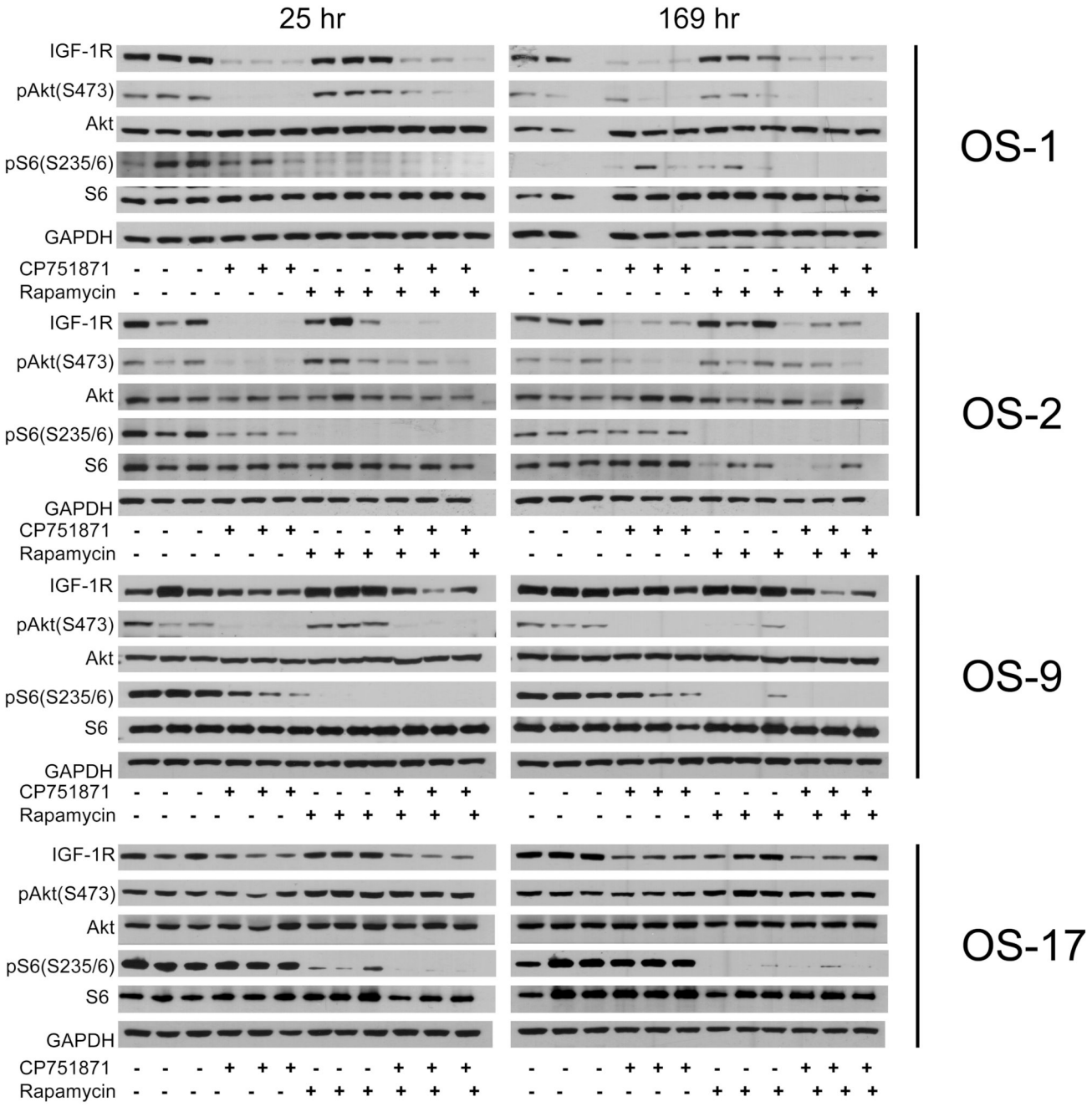


**Figure 4.**

Pharmacodynamic changes in osteosarcoma xenografts associated with treatment regimens

Mice received CP-751,871 (0.5 mg/mouse) twice weekly, rapamycin daily 5-days per week or the combination. Tumors were harvested 1 hr after rapamycin administration, and snap-frozen in liquid $N_2$. Extracts were prepared from tumor powders and processed as described in Experimental Procedures. For each condition (control, CP-751,871, rapamycin or the combination) 3 independent tumors were used at each time point.

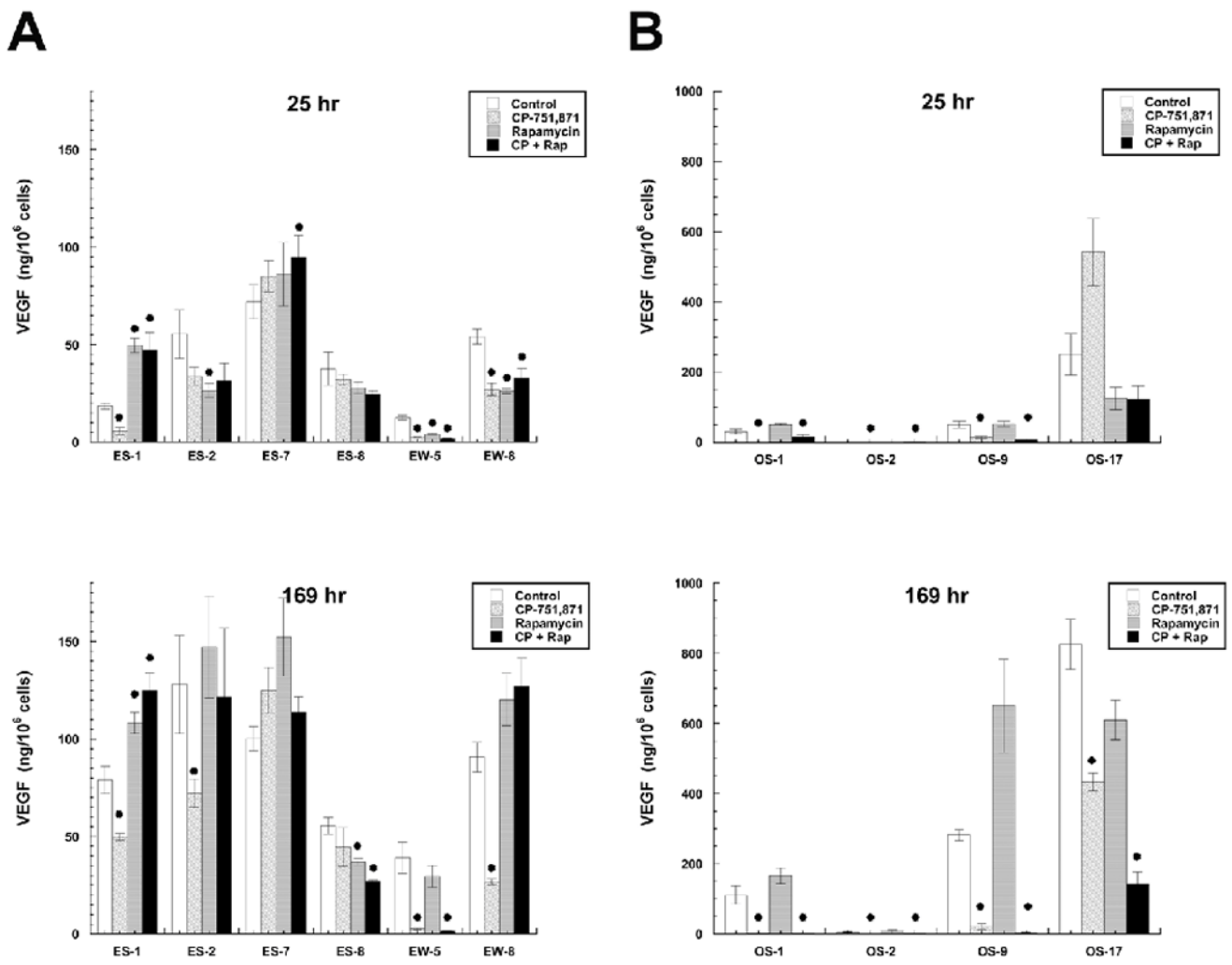


**Figure 5.**

VEGF levels in control and treated tumor xenografts

Mice received CP-751,871 (0.5 mg/mouse) twice weekly, rapamycin daily 5-days per week or the combination. Tumors were harvested 1 hr after the last dose of rapamycin, and snap-frozen in liquid $N_2$. Extracts were prepared from tumors and VEGF determined by a human-specific ELISA as described in Experimental Procedures. For each condition (control, CP-751,871, rapamycin or the combination) 6 to 9 independent determinations were used at each time point. * indicates significantly different from controls ($P<0.05$).

**A.** EWS xenografts.

**B.** OS xenografts.

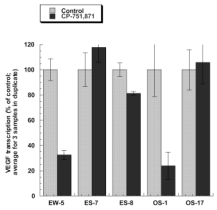


**Figure 6.**

VEGF gene expression in control and CP-751,871-treated tumor xenografts. Total RNA was extracted from the tumors 25 hr after administration of CP-751871, reverse transcribed to cDNA and further quantified by real-time RT-PCR as described in Experimental Procedures. The quantity of cDNA in each reaction was normalized to GAPDH and calculated as a ratio of sample cDNA to GAPDH cDNA. Each column represents an average value for duplicate determinations from 3 independent tumors (± SEM). Sample values were plotted in the histogram as per cent of control tumors (untreated). Control levels being set to 100% for each tumor line.